



Since January 2020 Elsevier has created a COVID-19 resource centre with free information in English and Mandarin on the novel coronavirus COVID-19. The COVID-19 resource centre is hosted on Elsevier Connect, the company's public news and information website.

Elsevier hereby grants permission to make all its COVID-19-related research that is available on the COVID-19 resource centre - including this research content - immediately available in PubMed Central and other publicly funded repositories, such as the WHO COVID database with rights for unrestricted research re-use and analyses in any form or by any means with acknowledgement of the original source. These permissions are granted for free by Elsevier for as long as the COVID-19 resource centre remains active.



## Delivery to the lower respiratory tract is required for effective immunization with Newcastle disease virus-vectored vaccines intended for humans

Joshua M. DiNapoli<sup>a</sup>, Jerrold M. Ward<sup>a</sup>, Lily Cheng<sup>a</sup>, Lijuan Yang<sup>a</sup>, Subbiah Elankumaran<sup>b,1</sup>, Brian R. Murphy<sup>a</sup>, Siba K. Samal<sup>b</sup>, Peter L. Collins<sup>a</sup>, Alexander Bukreyev<sup>a,\*</sup>

<sup>a</sup> Laboratory of Infectious Diseases, National Institute of Allergy and Infectious Diseases, National Institutes of Health, Bethesda, MD 20892-8007, USA

<sup>b</sup> Department of Veterinary Medicine, Virginia-Maryland College of Veterinary Medicine, University of Maryland, 8075 Greenmead Drive, College Park, MD 20742-3711, USA

### ARTICLE INFO

#### Article history:

Received 24 September 2008

Received in revised form 24 December 2008

Accepted 5 January 2009

Available online 23 January 2009

#### Keywords:

Virus  
Vaccine  
Vector  
Immunization  
Route of immunization  
Newcastle disease virus

### ABSTRACT

Newcastle disease virus (NDV), an avian virus, is being evaluated for the development of vectored human vaccines against emerging pathogens. Previous studies of NDV-vectored vaccines in a mouse model suggested their potency after delivery by injection or by the intranasal route. We compared the efficacy of various routes of delivery of NDV-vectored vaccines in a non-human primate model. While delivery of an NDV-vectored vaccine by the combined intranasal/intratracheal route elicited protective immune responses, delivery by the subcutaneous route or the intranasal route alone elicited limited or no protective immune responses, suggesting the necessity for vaccine delivery to the lower respiratory tract. Furthermore, direct comparison of a vaccine based on an NDV mesogenic strain (NDV-BC) with a similarly designed NDV vector based on a modified lentogenic strain carrying a polybasic F cleavage site (NDV-VF) suggested that the two NDV strains were similar in immunogenicity and were equally protective.

Published by Elsevier Ltd.

### 1. Introduction

The continuing outbreaks of emerging viral pathogens, such as highly pathogenic avian influenza virus, severe acute respiratory syndrome coronavirus (SARS-CoV), Ebola virus, and others demonstrate the need for effective vaccine systems that can be rapidly adapted to novel pathogens. Vectored vaccines are one of the most feasible approaches for achieving protection against infection with such pathogens [reviewed in [1]]. While the use of human viruses as vaccine vectors may be seriously hampered by pre-existing immunity to these viruses, development of vaccines based on antigenically distinct non-human viruses, such as vesicular stomatitis virus and Newcastle disease virus (NDV), may represent a viable alternative.

NDV is an avian pathogen and is a member of the *Avulavirus* genus of subfamily *Paramyxovirinae* of family *Paramyxoviridae*. NDV isolates can be divided into three groups based on their degree of

virulence in birds: (i) lentogenic strains, which cause mild or non-apparent infections that are largely limited to the respiratory or alimentary tract and which include strains presently in use as live vaccines for chickens; (ii) mesogenic strains, which can cause systemic infections of intermediate severity, but are also sometimes used for vaccination of poultry; and (iii) velogenic strains, which cause systemic infections with high mortality rates. A major determinant of NDV virulence in birds is the cleavage site of the F protein. In velogenic and mesogenic strains, the F cleavage site is polybasic, and cleavage is mediated by ubiquitous intracellular proteases such as furin. In lentogenic strains, the cleavage site contains fewer basic amino acids, and cleavage is dependent on secretory trypsin-like proteases present only in luminal fluids of the respiratory and alimentary tracts. Replacement of the F cleavage site of lentogenic strains with a polybasic site from a mesogenic strain results in a virus whose virulence is intermediate between that of the parental lentogenic strain and the mesogenic strain from which the cleavage site is derived [2,3].

In recent years, we and others have developed vaccine constructs for potential human use based on lentogenic and mesogenic NDV strains as well as lentogenic strains that were modified to contain a polybasic cleavage site [4]. In mice, intravenous (IV), intraperitoneal (IP) or intranasal (IN) immunization with these constructs resulted in a protective immune response [5–7]. However, because mice are phylogenetically and anatomically distinct from humans, it

\* Corresponding author at: LID, NIAID, NIH, 50 South Drive, Room 6505, Bethesda, MD 20892-8007, USA. Tel.: +1 301 594 1854; fax: +1 301 496 8312.

E-mail address: [abukreyev@nih.gov](mailto:abukreyev@nih.gov) (A. Bukreyev).

<sup>1</sup> Current address: Virginia-Maryland Regional College of Veterinary Medicine, Center for Molecular Medicine and Infectious Diseases, Virginia Polytechnic Institute and State University, Blacksburg, VA 24061, USA.

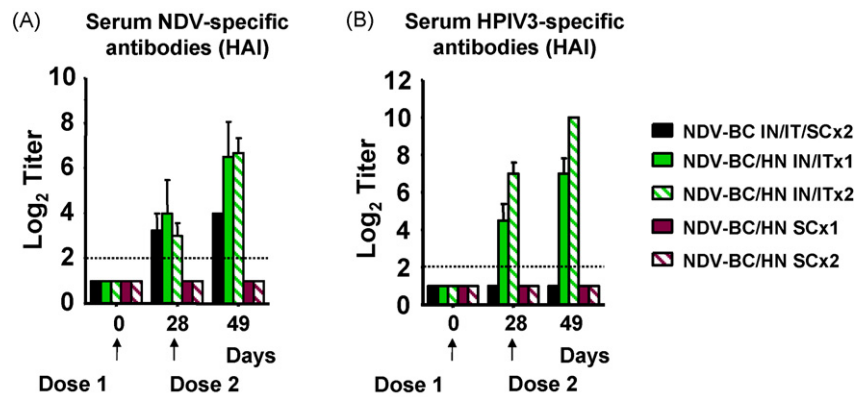


**Fig. 1.** Serum antibody responses following SC or IN/IT immunization of AGM with NDV-BC/HN. (A) NDV-specific and (B) HPIV3 HN-specific HAI serum antibody responses in monkeys following one or two doses of the indicated virus delivered by the SC or IN/IT route. The mean log<sub>2</sub> titer  $\pm$  SE is shown for each group. Dashed lines represent the limit of detection ( $2 \log_2$ ). Titers below the limit of detection were assigned a value of  $1 \log_2$  for calculation of the mean and SE. Each group contained 4 animals.

is unknown whether results obtained with in mice can be extrapolated to potential human use. In particular, the safety and efficacy of live NDV-vectored vaccines will depend on how well this avian virus replicates in the heterologous host, and it is unclear how the level of permissiveness in rodents would compare to that in primates. Additional studies in non-human primates, a model that is more relevant to potential human use, showed that, when administered by the combined IN and intratracheal (IT) routes, NDV is highly attenuated, well-tolerated, immunogenic, and protective [8–10], as reviewed in [4]. In the present study, we used a non-human primate model to compare various routes of immunization with NDV-vectored vaccines. In addition, we compared the immunogenicity and protective efficacy of an NDV-vectored vaccine based on a mesogenic strain of the virus with that based on a modified lentogenic strain carrying a polybasic F cleavage site in order to choose the vector representing the best balance of immunogenicity versus veterinary safety.

## 2. Materials and methods

### 2.1. The vaccine constructs

The NDV constructs were based on the mesogenic Beaudette C strain (NDV-BC) or on a virus called NDV-VF, which is a version of the lentogenic strain La Sota that was modified to bear the polybasic F cleavage site of NDV-BC and is intermediate in virulence between NDV-BC and NDV-La Sota [2,3]. We previously modified NDV-BC to express the hemagglutinin-neuraminidase (HN) protein of human parainfluenza virus type 3 (HPIV3), creating NDV-BC/HN, and previously modified NDV-BC and NDV-VF to express the spike glycoprotein (S) of SARS-CoV, creating NDV-VF/S and NDV-BC/S, respectively [8,10]. Briefly, the open reading frame encoding the HPIV3 HN protein (accession number Z11575.1) or the SARS-CoV S protein (accession number AAP13441.1) was amplified by PCR and inserted into the P/M junction of the NDV-BC or NDV-VF genome to be expressed as a separate mRNA. NDV recombinants were recovered and amplified in embryonated chicken eggs. Titers of the constructs were determined by plaque titration on monolayers of DF-1 chicken fibroblast cells in 24-well plates.

### 2.2. Immunization and challenge of African green monkeys

Adult African green monkeys (AGM) (*Cercopithecus aethiops*) confirmed to be seronegative for NDV and HPIV3 by hemagglutination inhibition (HAI) assay using turkey and guinea pig erythrocytes were used in two studies. IN and IT immunizations were performed as previously described [11]. In the first study (Fig. 1), AGM were immunized with NDV-BC/HN by the combined IN and IT routes or

by the subcutaneous (SC) route, at a dose of  $10^7$  PFU per site. On day 28, animals received a second dose by the same route(s) of either the same construct or the parental NDV-BC lacking an insert. As a negative control, an additional group was immunized on days 0 and 28 with NDV-BC empty vector administered IN, IT, and SC, at a dose of  $10^7$  PFU per site. This resulted in a total of 4 experimental groups and one control group (see Fig. 1) that each contained 4 animals. Serum samples were collected on days 0, 28, and 49 to assess vector- and insert-specific immune responses.

In the second study (Figs. 2–6 and Table 1), AGM were immunized by the combined IN and IT routes on days 0 and 28 with  $10^7$  PFU per site of NDV-BC empty vector (2 animals), NDV-BC/S (4 animals), or NDV-VF/S (4 animals), or with  $10^7$  PFU of NDV-BC/S by the IN route (4 animals). Vaccine virus shedding was determined in tracheal lavage (TL) samples taken on days 2, 4, and 6 after the first dose as previously described [11]. To assess serum and mucosal antibody responses, serum, nasopharyngeal wash (NW), and TL samples were collected on days 0, 14, 21, 28, 42, 49, and 56 as previously described [11]. To assess the protective efficacy of the vaccines, all animals in study two were challenged on day 56 by the combined IN and IT routes with  $10^6$  50%-tissue-culture-infectious-dose-units (TCID<sub>50</sub>) of SARS-CoV per site, as previously described [11]. NW and TL samples were collected on days 1 and 2 post-challenge to measure challenge SARS-CoV shedding. Two days post-challenge, animals were sacrificed and triplicate  $\sim 1 \text{ cm}^3$  sam-

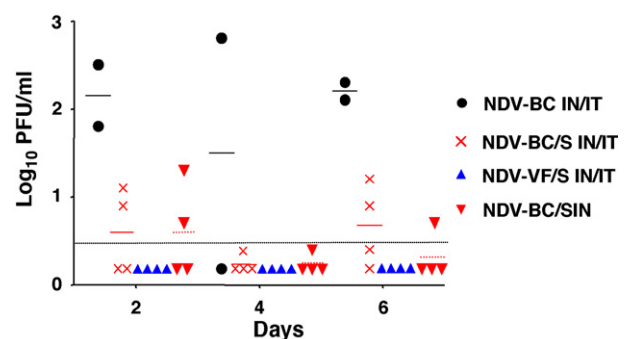


**Fig. 2.** NDV vector shedding following IN or IN/IT immunization of AGM with NDV-BC, NDV-BC/S or NDV-VF/S. TL samples were taken on days 2, 4, and 6 following administration of the indicated NDV construct on day 0. The NDV titer in each sample was determined by plaque titration on monolayers of DF-1 cells. The individual value for each animal is plotted (the NDV-BC control group contained 2 animals; the other groups contained 4 animals each), with the group mean indicated by a horizontal bar. The dotted line represents the limit of detection ( $0.4 \log_{10}$  PFU/ml). Values below the limit of detection were assigned a value of  $0.2 \log_{10}$  PFU/ml. This experiment is continued in Figs. 3–6 and Table 1.

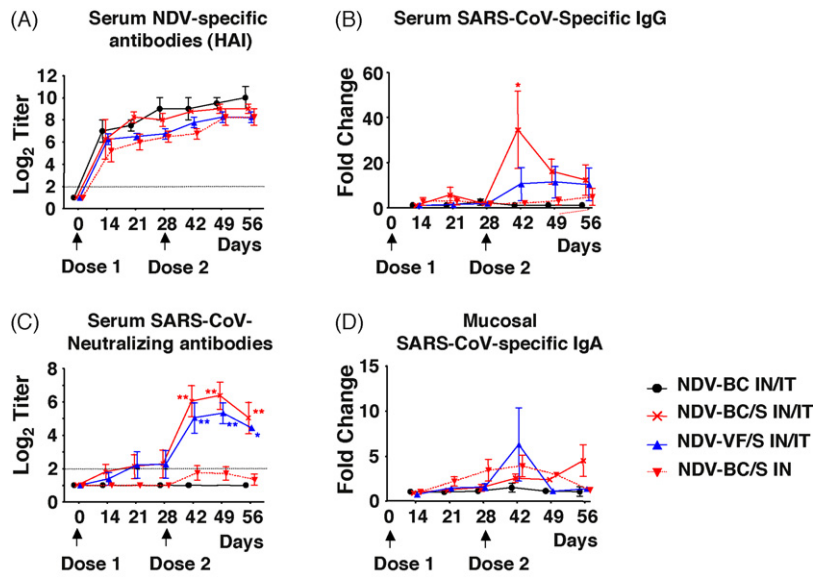


**Fig. 3.** Serum and mucosal antibody responses following IN or IN/IT immunization of AGM on days 0 and 28 with NDV-BC, NDV-BC/S or NDV-VF/S. (A) NDV-specific HAI serum antibody responses; mean titer  $\pm$  SE for each group. Values below the limit of detection ( $2 \log_2$ , dotted line) were assigned a value of  $1 \log_2$  for calculations. (B) SARS-CoV-specific serum IgG responses evaluated by ELISA with purified SARS-CoV S as an antigen; mean fold increase relative to day 0  $\pm$  SE for each group. The value for each animal was recorded as the  $\log_2$  of the serum dilution resulting in an absorbance at 450 nm that was more than double the background and greater than 0.3. Values below the limit of detection were assigned a value of  $2 \log_2$ . At day 0, the mean background  $\log_2$  titer for each group was as follows: NDV-BC IN/IT, 2.0; NDV-BC/S IN/IT, 4.3; NDV-VF/S IN/IT, 4.8, NDV-BC/S IN, 2.5. *P* values were calculated using a repeated measures two-way ANOVA with a Bonferroni post hoc analysis compared to the value for the NDV-BC IN/IT (control) group at the same time point: \**P* < 0.01. (C) SARS-CoV-neutralizing serum antibody responses; mean  $\log_2$  titer  $\pm$  SE for each group. Values below the detection limit ( $2 \log_2$ , dotted line) were assigned a value of  $1 \log_2$ . *P* values were calculated using a repeated measures two-way ANOVA with a Bonferroni post hoc analysis compared to the value for the NDV-BC IN/IT (control) group at the same time point: \**P* < 0.01; \*\**P* < 0.001. Note: the titer was not determined for the NDV-BC IN/IT group on days 21 and 49. At these time points, the *P* values for the other groups were calculated using the day 0 value for the NDV-BC IN/IT group. (D) SARS-CoV-specific mucosal IgA responses; mean increase relative to day 0  $\pm$  SE fold for each group. TL samples were collected and concentrated 20–30-fold. They were then analyzed in an IgA isotype-specific ELISA against purified SARS-CoV S starting at a dilution of 1:10 ( $3.3 \log_2$ ). The value for each animal was recorded as the  $\log_2$  of the serum dilution resulting in an absorbance at 450 nm that was more than double the background and greater than 0.1. Values below the limit of detection were assigned a value of  $2.3 \log_2$ . To account for variability in sample collection and concentration, the titers were then normalized to the total IgA mass in each sample, as determined in a quantitative total IgA ELISA. At day 0, the mean normalized  $\log_2$  background titer for each group was as follows: NDV-BC IN/IT, 1.7; NDV-BC/S IN/IT, 1.8; NDV-VF/S IN/IT, 2.0, NDV-BC/S IN, 1.7.

ples were taken from seven regions of the lung: the left hilar region, the left upper and lower lobes, the right hilar region, and the right upper, middle and lower lobes. One sample from each tissue was fixed in 10% neutral buffered formalin for immunohistochemical (IHC) and histopathological analysis. The remaining two samples from each organ were homogenized in L-15 medium (Invitrogen, Carlsbad, CA, USA) to achieve a final concentration of 10% (w/v). SARS-CoV titers in the supernatant were determined by titration as described below.

All primate experiments were performed at Bioqual, Inc. (Rockville, MD, USA), a site approved by the Association for Assessment and Accreditation of Laboratory Care International with a protocol approved by the Animal Care and Use Committee of the NIAID.

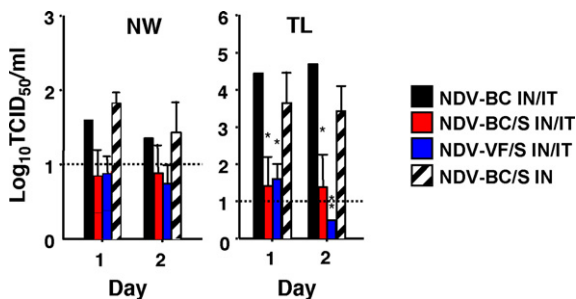


**Fig. 4.** SARS-CoV challenge virus replication in animals immunized on days 0 and 28 by the IN or the IN/IT routes with NDV-BC, NDV-BC/S or NDV-VF/S; SARS-CoV shedding in respiratory secretions. The animals were challenged with SARS-CoV on day 56, and NW and TL samples were collected on days 1 and 2 post-challenge and analyzed by virus titration in Vero cells. The mean  $\log_{10}$  titer  $\pm$  SE for each group is shown. The limit of detection ( $1 \log_{10}$  TCID<sub>50</sub>/ml) is shown by the dotted line; samples below the limit were assigned a value of  $0.5 \log_{10}$ . Mean  $\pm$  SE values are shown. *P* values were calculated by comparing the mean titer of the experimental group to that of the control group using a repeated measures two-way ANOVA with a Bonferroni post hoc analysis: \**P* < 0.05, \*\**P* < 0.01.

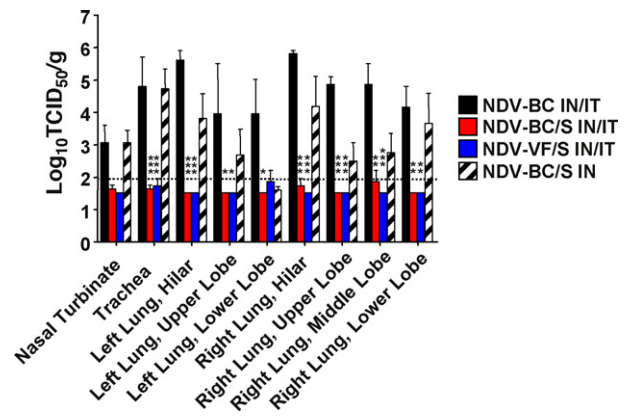


**Fig. 5.** SARS-CoV challenge virus replication in animals immunized on days 0 and 28 by the IN or the IN/IT routes with NDV/BC, NDV-BC/S or NDV-VF/S; direct quantitation of SARS-CoV challenge virus in respiratory tract tissue samples (this is a continuation of the experiment shown in Fig. 4). The animals were challenged with SARS-CoV on day 56. They were then euthanized on day 2 post-challenge and tissue samples were taken from the indicated regions. Duplicate tissue samples from each animal were homogenized and the viral titers were determined. The mean  $\log_{10}$  titer  $\pm$  SE for each group is shown. The limit of detection ( $2 \log_{10}$ ) is indicated by a dotted line; titers below the limit were assigned a value of  $1.5 \log_{10}$  TCID<sub>50</sub>/g. Mean  $\pm$  SE values are shown. *P* values were calculated by comparing the mean titer of the experimental group to that of the control group using a repeated measures two-way ANOVA with a Bonferroni post hoc analysis: \**P* < 0.05, \*\**P* < 0.01, \*\*\**P* < 0.001.

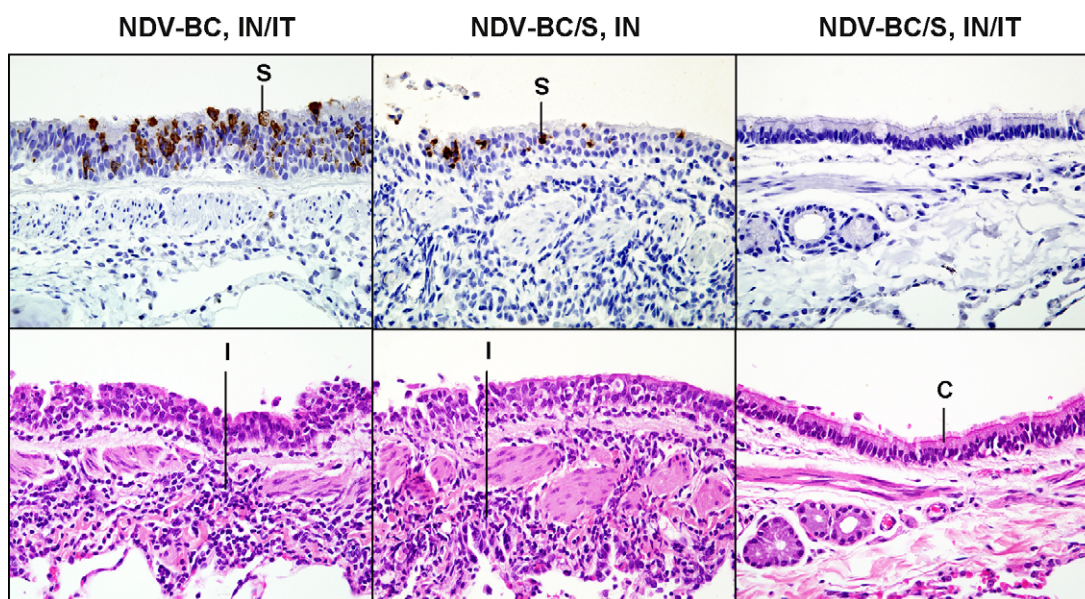


**Fig. 6.** SARS-CoV challenge of animals immunized on days 0 and 28 by the IN or the IN/IT routes with NDV-BC or NDV-BC/S: IHC and histopathological analysis of the lung tissues harvested 2 days following challenge with SARS-CoV on day 56 (this is a continuation of the experiment shown in Figs. 4 and 5). All micrographs were captured at 400 $\times$  magnification. Top row: IHC detection of SARS-CoV N protein (S). A significant number of antigen-positive cells are seen in the vector control (left panel), but not the animals immunized with NDV-BC/S by the IN/IT routes (right panel). Antigen-positive cells are also present in animals immunized with NDV-BC/S by the IN route, although at a reduced number (middle panel). Bottom row: Hematoxylin and eosin staining. Features characteristic of SARS-CoV pathogenesis were noted in animals that had been immunized with the empty vector (left panel) or NDV-BC/S by the IN route (middle panel), including marked cellular infiltration (I) of the interstitium and lining epithelium by primarily neutrophils and lymphocytes. In addition, the cilia (C) that are evident in animals previously immunized with NDV-BC/S IN/IT (right panel) are largely absent in animals immunized with the empty vector or with NDV-BC/S IN. Overall, no significant pathological changes were observed in the animals immunized with NDV-BC/S by the IN/IT routes (right panel), whereas animals immunized with NDV-BC/S by the IN route (middle), pathological changes similar to those observed in the empty vector control animal (left) are seen.

### 2.3. Virological and serological assays

NDV titers were determined by plaque titration on monolayers of DF-1 cells. Infected monolayers were covered with methylcellulose overlay, incubated at 37 $^{\circ}$ C for 4 days and stained with a crystal violet solution. HPIV3 titers were determined by plaque titration on monolayers of LLC-MK2 rhesus monkey kidney cells. Infected monolayers were covered with methylcellulose overlay and incubated at 37 $^{\circ}$ C for 5–6 days. Thereafter, the monolayers were fixed, and the plaques were immunostained with a rabbit anti-serum raised against purified HPIV3 virions and a goat anti-rabbit secondary antibody conjugated to horseradish peroxidase (KPL, Gaithersburg, MD). The plaques were then visualized using the 4CN 2-component peroxidase substrate (KPL, Inc., Gaithersburg, MD, USA) and counted. SARS-CoV titers (TCID<sub>50</sub>/ml) were determined by limiting dilution on monolayers of Vero cells and examination of visible cytopathology on days 3 and 4 post-infection. The 50% endpoint was calculated by the method of Reed and Muench [12].

In studies assessing plaque size of NDV-BC at various temperatures, NDV inocula were serially diluted in medium and were then used to infect replicate 24-well plates of DF-1 and LLC-MK2 cells at 37 $^{\circ}$ C. After 1 h, the wells received overlay medium containing 0.8% methylcellulose and the plates were incubated for 4 days (DF-1 cells) or 12 days (LLC-MK2 cells) at the indicated temperatures. For the DF-1 cells, the monolayers were stained with crystal violet and plaques were counted. For the LLC-MK2 cells, the monolayers were fixed and the plaques were immunostained using a chicken anti-NDV primary antibody (Charles River Labs, Wilmington, MA, USA) and a rabbit anti-chicken horseradish peroxidase conjugate secondary antibody (Jackson ImmunoResearch Laboratories, Inc., West Grove, PA, USA). The plaques were then visualized using the 4CN 2-component peroxidase substrate (KPL, Inc., Gaithersburg, MD, USA) and counted. For evaluation of plaque size of HPIV3 in LLC-MK2 cells, the monolayers were infected, covered with medium

containing 0.8% methylcellulose, incubated at 32 $^{\circ}$ C or 37 $^{\circ}$ C for 10 days, and the plaques were stained as above. The plaque diameters (in pixels) were calculated by analysis of digitized images using Adobe Photoshop CS3 Extended (Adobe, San Jose, CA, USA).

To assess the growth kinetics of viruses at 32 $^{\circ}$ C or 39 $^{\circ}$ C, triplicate monolayers of LLC-MK2 cells in 12-well plates were infected at a multiplicity of infection per cell (MOI) of 5 PFU for analysis of single-step growth or an MOI of 0.001 PFU for analysis of multi-step growth. After a 1-h incubation at the indicated temperature, the wells were washed 3 times with growth medium and then overlaid with 1 ml per well of growth medium. At each time point, 100  $\mu$ l of medium was removed from each well and replaced with 100  $\mu$ l of fresh medium. The virus titer at each time point was determined by plaque titration as described above.

To analyze antigen expression following infection at 32 $^{\circ}$ C or 39 $^{\circ}$ C, LLC-MK2 cell monolayers were infected at an MOI of 5 or 0.001 PFU with NDV-BC, NDV-BC/S, or HPIV3. The monolayers were lysed at various time points by addition of 1 $\times$  NuPAGE LDS sample buffer (Invitrogen) containing 5%  $\beta$ -mercaptoethanol directly to the cells. The lysates were then denatured at 70 $^{\circ}$ C for 10 min and separated by SDS-PAGE using NuPAGE Novex 4–12% bis tris gels (Invitrogen). The gels were then analyzed by Western blotting using a polyvinylidene fluoride membrane (Invitrogen) and either a chicken polyclonal antibody directed against NDV (Charles River Laboratories International, Inc., Germantown, MD, USA) or a rabbit polyclonal antibody against  $\beta$ -actin (Abcam, Cambridge, MA, USA).

NDV-specific and HPIV3-specific serum antibody titers were determined by HAI assay using turkey or guinea pig erythrocytes, respectively, as previously described [10]. Antibodies specific for the SARS-CoV S protein were detected by either IgA or IgG isotype-specific ELISA as previously described [8,11]. Prior to ELISA, NW and TL samples were concentrated 20–30-fold to a final volume of  $\sim$ 0.5 ml using Vivaspin 30,000 molecular weight cutoff columns (Sartorius Corp., Edgewood, NY, USA). To account for differences in

**Table 1**

Immunohistochemical and histopathological characterization of lung tissue samples from African green monkeys that were immunized with NDV-vectored vaccines and challenged with SARS-CoV<sup>a</sup>.

Immunizing virus; route of immunization	Animal ID#	SARS-CoV antigen <sup>b</sup>			Pathology <sup>c</sup>			
		Bronchial	Bronchiolar	Interstitial	Bronchial/Bronchiolar inflammation	Bronchial/Bronchiolar necrosis	Peribronchial/ Perivascular cuffing	Interstitial inflammation
NDV-BC IN/IT (control)	1	++	+/-	+	+	+/-	+	+
	2	+	+/-	+	+	-	+/-	+/-
	3	-	-	-	-	-	+	+
NDV-BC/S IN/IT	4	-	-	-	-	-	-	+
	5	-	-	-	-	-	+	+/-
	6	+	+/-	+/-	-	-	-	-
NDV-VF/S IN/IT	7	+/-	-	-	-	-	-	-
	8	-	-	-	-	-	-	+/-
	9	-	-	-	-	-	-	-
	10	-	-	-	+/-	-	-	-
NDV-BC/S IN	11	+	-	-	+/-	-	+/-	+/-
	12	+/-	-	-	+/-	+/-	+/-	+
	13	+	+	+/-	+/-	+/-	-	+/-
	14	+	-	+	+/-	+/-	-	+/-

<sup>a</sup> Animals were immunized on days 0 and 28 with the indicated NDV constructs by the IN or IN/IT routes at a dose of  $10^7$  PFU per site. The animals were challenged on day 56 by the combined IN/IT routes with  $10^6$  TCID<sub>50</sub> of SARS-CoV per site. The animals were sacrificed on day 2 post-challenge and tissue specimens were obtained from left lung hilum, left lung upper lobe, left lung lower lobe, right lung hilum, right lung upper lobe, right lung middle lobe, and the right lung lower lobe. Bronchial, bronchiolar, interstitial, and vascular structures within these specimens were inspected microscopically.

<sup>b</sup> IHC analysis was performed on tissue sections from three lung regions, namely the left lung hilum, right lung hilum, and right lung middle lobe. Antigen staining was scored as follows: ++, multiple clusters of antigen-positive cells in multiple tissue sections; +, single cells stained in multiple tissue sections; +/-, antigen-positive cells detected in a single tissue section; -, no antigen detected.

<sup>c</sup> Histopathological analysis was performed on tissues sections stained with hematoxylin and eosin. Pathological features of infection were scored as follows: +, pathological feature detected in 4 or more lung sections; +/-, positive in 2 or 3 lung sections; -, positive in 0 or 1 lung section.

sample collection and processing, NW and TL IgA titers were normalized to total IgA content in each sample as previously described [9]. We also performed SARS-CoV neutralization assays on serum samples as previously described [8]. All experiments involving infectious SARS-CoV were done under biosafety level 3 conditions.

#### 2.4. IHC and histopathological analysis of tissues

Fixed tissue samples were embedded in paraffin, sectioned at 4–6  $\mu\text{M}$ , and used for hematoxylin and eosin staining or for immunostaining of SARS-CoV antigen. For IHC analysis, tissue sections first were treated with a food steamer and Diva solution (Biocare, Concord, CA, USA) to retrieve antigen. SARS-CoV antigen was visualized by immunostaining with a mouse monoclonal antibody to SARS-CoV nucleoprotein N (Abcam, Cambridge, MA, USA) at a dilution of 1:100, followed by treatment of sections with the Dako Envision + mouse polymer link (Dako, Carpinteria, CA, USA) with diaminobenzidine as the chromogen.

### 3. Results

#### 3.1. NDV-vectored vaccines require respiratory tract delivery

We first compared NDV vaccine immunogenicity when administered by either the combined IN/IT routes or the SC route. AGM (four animals per group) were inoculated with one or two doses (28 days apart) of an NDV-BC vector expressing the HN protein of HPIV3 (NDV-BC/HN) [10] by either the combined IN/IT route or by the SC route (Fig. 1). An additional group of 4 animals received the empty NDV-BC vector by the combined IN/IT and SC routes. Serum samples were collected on days 28 and 49, which were 28 days after the first dose and 21 days after the second dose, and analyzed by HAI for the presence of antibodies specific to the NDV vector and to the HPIV3 HN insert. Only animals that received an NDV construct by the combined IN/IT route had detectable NDV-specific antibodies (Fig. 1A). Neither one nor two doses of NDV-BC/HN administered by the SC route resulted in a detectable NDV HAI response. A similar result was obtained for the HPIV3-specific response, as either one or two doses of NDV-BC/HN administered by the combined IN/IT routes induced HPIV3-specific HAI titers (Fig. 1B). Again, SC delivery of the vaccine construct failed to elicit a detectable HPIV3-specific antibody response.

#### 3.2. Lower respiratory tract delivery is required for effective immune response to NDV-vectored vaccines

In a second study, we compared the level of replication, immunogenicity and protective efficacy of NDV vaccines delivered by the combined IN/IT routes or by the IN route alone (Figs. 2–6 and Table 1). We have previously shown that NDV-BC expressing the S protein of SARS-CoV (NDV-BC/S) induced a protective immune response in AGM when delivered by the combined IN/IT routes [8]. In the present study, we immunized AGM with the NDV-BC empty vector by the IN/IT routes (2 animals) or with NDV-BC/S by the IN/IT routes (4 animals) or by the IN route only (4 animals). Four additional animals were immunized by the IN/IT routes with NDV-VF/S, which is a version of the lentogenic La Sota strain that contains the polybasic F cleavage site of NDV-BC and was engineered to express the SARS-CoV S protein [8]. On day 28 after the first immunization, all animals received a second dose of the same construct by the same route. TL samples were obtained after the initial vaccine dose to assess vector shedding (Fig. 2). The shedding of NDV-BC/S was reduced compared to the NDV-BC empty vector, suggesting that insertion of the SARS-CoV S ORF attenuated *in vivo* replication (Fig. 2). We also detected a lower level of shedding in animals immunized with NDV-BC/S by the IN route, suggesting that this route

resulted in a reduced level of replication. Shedding was not detected in animals immunized with NDV-VF/S, suggesting a greater level of attenuation of the NDV-VF versus NDV-BC-based constructs.

Serum samples were collected on days 14, 21, 28, 42, 49, and 56 (i.e., 14, 21, and 28 days after the first and second vaccine doses) and analyzed for NDV-specific antibodies by HAI assay, for SARS-CoV-specific IgG by ELISA, and for SARS-CoV-specific neutralizing antibodies as previously described [13] (Fig. 3, panels A–C). In addition, the mucosal antibody response was analyzed by quantitation of SARS-CoV-specific IgA in TL samples (Fig. 3, panel D). We detected NDV-specific serum antibody titers beginning at day 14 after the first dose, which gradually increased at the later time points (Fig. 3A). The highest titers were detected in the NDV-BC IN/IT group, followed in order by NDV-BC/S IN/IT, NDV-VF/S IN/IT and NDV-BC/S IN. The SARS-CoV-specific serum IgG titers were at background levels in all immunized groups after the first dose (Fig. 3B). After the second dose, high titers were detected in 4 of 4 animals in the NDV-BC/S IN/IT and 3 of 4 animals in the NDV-VF/S IN/IT groups, with greater antibody levels in the former group on days 42 and 49. In contrast, after immunization by the IN route only, the IgG titers remained at background level. Similar to what was observed for the IgG responses, substantial SARS-CoV-neutralizing serum antibody responses were detected after the second dose in all 8 animals immunized by the combined IN/IT route with NDV-BC/S or NDV-VF/S, but not in animals immunized by the IN route alone with NDV-BC/S (Fig. 3C). Again, NDV-BC/S induced a greater response, as compared to NDV-VF/S. We also observed an increase in SARS-CoV-specific IgA titer in the TL samples of most of the animals that received vaccine by either the combined IN/IT route or the IN route alone (Fig. 3D). Specifically, all 4 animals that received NDV-BC/S by the combined IN/IT route demonstrated a 3–4-fold increase in TL IgA titer by day 42 that was maintained or increased through day 56. The TL IgA response was less consistent in the NDV-VF/S group, in which only 2 of 4 animals demonstrated a 5- and 18-fold increase in TL IgA on day 42 that had largely waned by day 56. Despite the relatively meager humoral responses, all 4 animals that received NDV-BC/S by the IN route alone demonstrated a 2–7.5-fold increase in S-specific TL IgA that was largely maintained through day 49, but returned to near background levels by day 56. We were unable to detect statistically significant differences between the groups due to the high animal-to-animal variability.

To evaluate protective efficacy of IN/IT versus IN immunization as well as NDV-BC/S versus NDV-VF/S, the animals were challenged on day 56 by the combined IN/IT routes with  $10^6$  TCID<sub>50</sub> of SARS-CoV per site. On days 1 and 2 post-challenge, NW and TL samples were collected to evaluate viral shedding (Fig. 4), and on day 2 the animals were euthanized and respiratory tract tissues were collected to assess SARS-CoV replication by quantitative virology (Fig. 5), IHC, and histopathologic analysis (Fig. 6). In the control animals, high or moderate titers of SARS-CoV challenge virus were detected in NW and TL samples (Fig. 4) and in respiratory tract tissues (Fig. 5), SARS-CoV antigen was easily detectable by IHC of lung tissue (Fig. 6 top row; Table 1). In the animals immunized by NDV-BC/S or NDV-VF/S by the combined IN/IT route, very little or no SARS-CoV was detected by any of the three methods. In contrast, the group immunized with NDV-BC/S by the IN route alone had a level of SARS-CoV shedding that was indistinguishable from that in the control group, and the titer of SARS-CoV detected by direct analysis of lung tissue was largely indistinguishable from that in the control group in most locations, with a modest reduction seen in some sections. Moreover, the level of viral antigen, as evaluated by IHC, was only marginally reduced as compared to the control group. Histopathological examination of bronchial tissues demonstrated a pronounced loss of cilia and increases in cellular infiltration and necrosis and/or apoptosis of bronchial epithelial cells following challenge of the NDV-BC con-

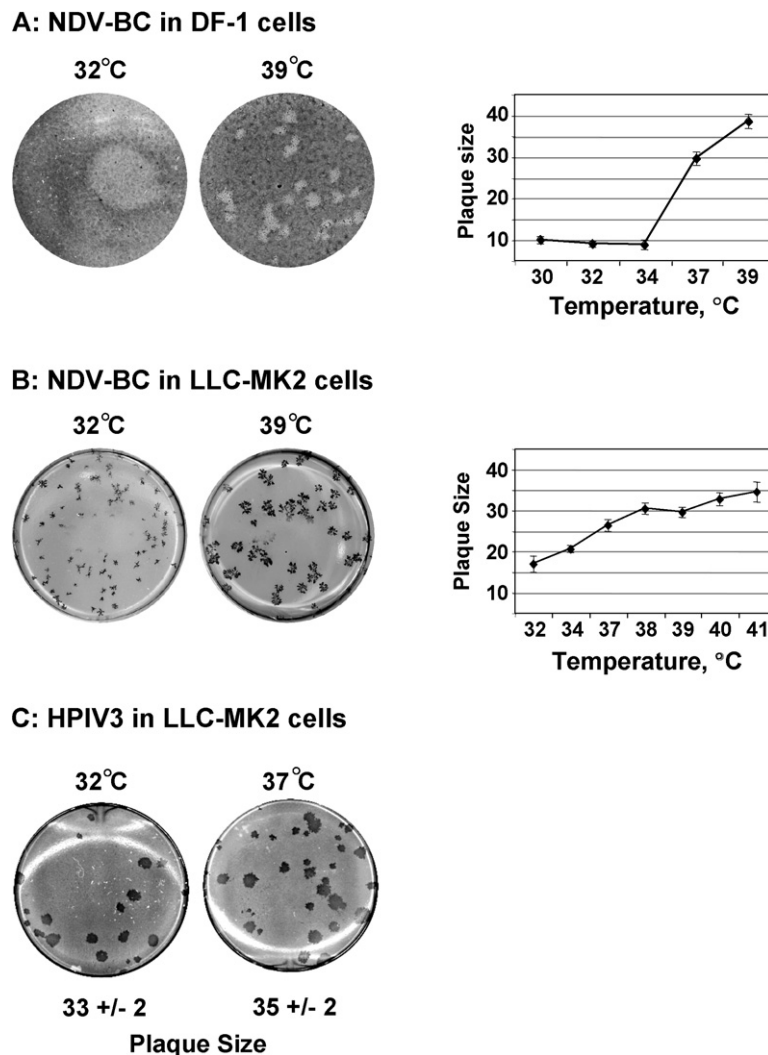


**Fig. 7.** Effect of temperature on plaque formation by NDV-BC. Monolayers of DF-1 (A) and LLC-MK2 (B and C) cells were infected with serial dilutions of NDV-BC (A and B) or HPIV3 (C) and incubated under methylcellulose at the indicated temperatures for 4 (Part A), 10 (part B), and 12 (part C) days. The monolayers were fixed and stained with crystal violet (DF-1 cells), immunostained with anti-NDV antibodies (NDV, LLC-MK2 cells), or immunostained with anti-HPIV3 antibodies (HPIV3). Plaque size was measured using Adobe Photoshop CS2 Extended software. Mean plaque sizes (pixels) ± SE, based on 10 plaques per virus per each temperature are shown.

tol as well as in the NDV-BC/S IN-immunized group, while little or no pulmonary pathology was detected in the IN/IT-immunized groups (Fig. 6, bottom row; Table 1, NDV-VF/S not shown).

### 3.3. NDV has a reduced ability to grow at the lower temperatures of the upper respiratory tract

Since NDV is an avian pathogen, we hypothesized that the virus may replicate more efficiently at the normal body temperature of the chicken, which is 40–41 °C, than at the body temperature of humans or African green monkeys, which is 37 °C and ~38–39 °C, respectively, or at the temperature of mucosa of the human nasal cavity, which is 32–34 °C [14]. We therefore infected monolayers of DF-1 chicken embryo fibroblast cells and LLC-MK2 monkey kidney cells with serial dilutions of NDV-BC and incubated the monolayers under methylcellulose at various temperatures for 4 and 12 days, respectively (Fig. 7A and B). Following incubation, the plaques were visualized as described in Section 2 and the plaque sizes and numbers were determined. Within the range of the temperatures tested, no significant difference in the viral titer was observed (data not shown). However, a dramatic reduction of the plaque size associated with the reduced temperatures was observed in the DF-1

chicken cells and, to a lesser degree, in LLC-MK2 monkey cells (Fig. 7A and B). For example, comparison of plaques sizes at 39 and 32 °C demonstrated a 77% reduction in size in DF-1 cells and a 43% size reduction in LLC-MK2 cells, suggesting significantly reduced virus growth at lower temperatures. A similarly significant difference was observed when plaques formed at 37 and 32 °C were compared (Fig. 7A and B). In contrast, the plaque size of HPIV3, a human respiratory pathogen, was equal at 37 and 32 °C (Fig. 7C).

We next compared growth kinetics of NDV-BC; NDV-BC/S and HPIV3 in LLC-MK2 cells at 32 and 39 °C after infection at an MOI of 5 PFU (Fig. 8A) or 0.001 PFU (Fig. 8B). Following infection at either MOI, replication of NDV-BC and NDV-BC/S was substantially reduced at 32 °C, as compared to 39 °C. In contrast, replication of HPIV3 was not significantly different at the two temperatures at most of the time points. In a separate set of experiments we compared NDV antigen production at 32 °C or 39 °C following infection at an MOI of 5 PFU (single-step growth) (Fig. 9A) or 0.001 PFU (multi-step growth) (NDV-BC, Fig. 9B; NDV-BC/S, Fig. 9C). At an MOI of 5, a 24 h-long incubation at 32 °C clearly resulted in a much lower level of the antigen expression, as compared to 39 °C (Fig. 9A). The low MOI (0.001 PFU) infection resulted in no detectable viral antigen at 24 h regardless of temperature (Fig. 9B and C). How-

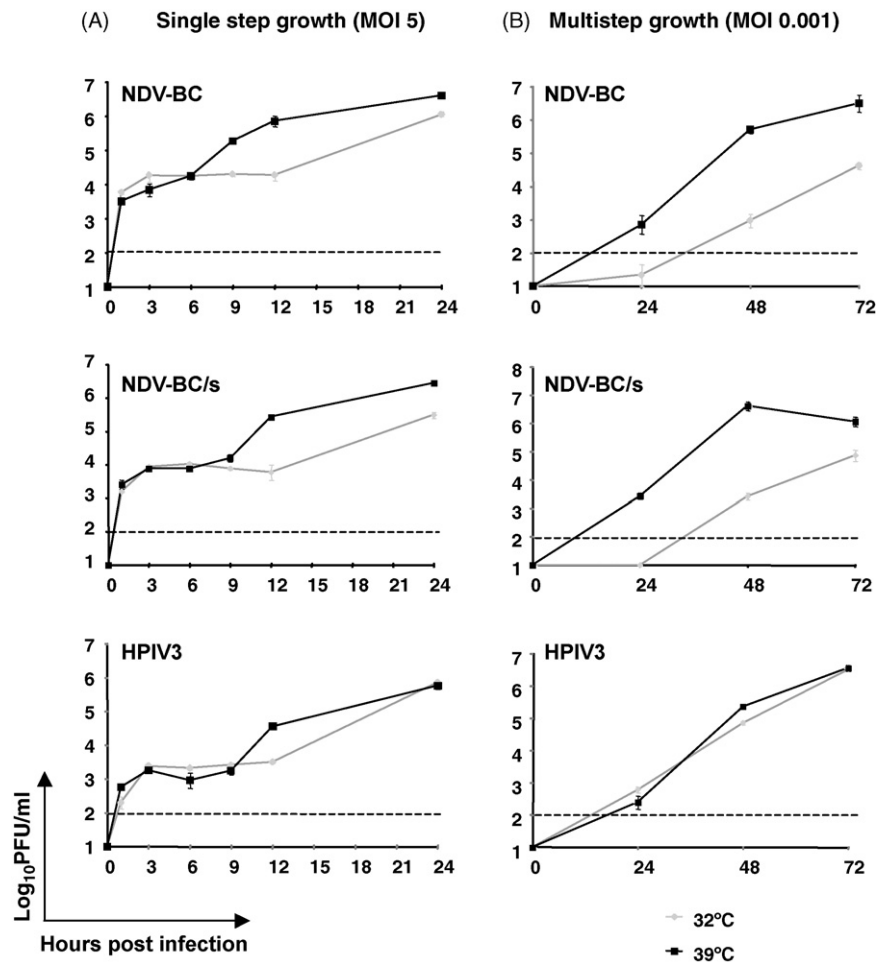


**Fig. 8.** Growth kinetics of NDV-BC, NDV-BC/S and HPIV3 in LLC-MK2 cells infected at an MOI of 5 PFU/cell (A) or 0.001 PFU/cell (B) at 32 and 39 °C. Triplicate monolayers of LLC-MK2 cells were infected at the indicated MOI and the virus present in the supernatant was titered at various time points post-infection. The titers were recorded as the  $\log_{10}$  PFU/ml  $\pm$  standard error.

ever, at 48 h there was abundant antigen in cell incubated at 39 °C, but no detectable expression of NDV in cells incubated at 32 °C. Moreover, we observed reduced antigen accumulation at 72 h in cells incubated at 32 °C. Taken together, these data indicate that, at the reduced temperatures of the upper respiratory tract of African green monkeys, the ability of NDV to replicate and produce viral antigen is greatly reduced.

#### 4. Discussion

These data represent the first direct comparison of immunogenicity and protective efficacy of NDV-vectored vaccine constructs following inoculation by various routes in a non-human primate model. These data suggest that (i) NDV-vectored vaccines require delivery through the respiratory tract, and that parenteral delivery by injection, even with two doses, is ineffective, (ii) for effective respiratory tract immunization, IT delivery is required, and (iii) a mesogenic strain of NDV is only marginally more immunogenic than a modified lentogenic strain containing a polybasic F cleavage site, and the two strains are equally protective. Previously published data in a mouse model demonstrated high immunogenicity and protective efficacy of an NDV-vectored vaccine administered by the IV and IP routes [5]. Although we did not test these particular routes of immunization (because they would not be appropriate for human use), the lack of any detectable response even after two doses delivered by the SC route suggests that delivery through the respiratory tract is a requirement for the immunogenicity of NDV-

vectored vaccines in primates. Another study utilizing the mouse model demonstrated greater immunogenicity and protective efficacy with IN immunization, as compared to IV or IP administration [6]. However, as opposed to the primate model, IN inoculation of mice typically results in delivery to both the upper and lower respiratory tract. For example, IN inoculation of 4-week-old BALB/c mice with a 20  $\mu$ l or 100  $\mu$ l inoculum resulted in delivery of 56% or 81%, respectively, of the inoculum to the lungs [15]. Therefore the mouse model does not allow a distinction between vaccine delivery to the upper and lower respiratory tract. Furthermore, the already noted low phylogenetic and anatomic relatedness between the mouse and human necessitate the use of more relevant models for assessment of the optimal routes of delivery for an NDV-vectored vaccine.

The complete lack of a detectable immune response to the NDV-vectored vaccine administered by injection might be explained by a tropism of the virus for the epithelial tissues of the respiratory tract, and hence restriction of replication to this site. However, the lack of significant immunogenicity after IN vaccination alone was surprising. IN delivery has been successfully used to vaccinate humans and non-human primates against human influenza viruses [16], respiratory syncytial virus [17], parainfluenza viruses [18], and vaccinia virus [19]. Why does IN immunization with NDV result in a different outcome? We note that infection of humans or non-human primates with live attenuated vaccines against human influenza virus, respiratory syncytial virus, and parainfluenza viruses results in efficient viral replication in both the upper and lower respiratory tract [17,22–24]. In contrast, direct analysis of the respiratory tract

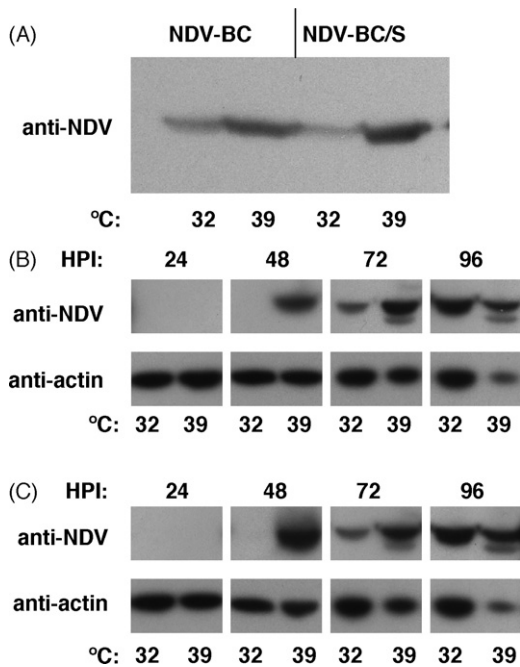


**Fig. 9.** Expression of NDV antigen in infected LLC-MK2 cells incubated at 32 °C or 39 °C at (A) 24 h after infection with NDV-BC or NDV-BC/S at MOI of 5 PFU, or (B and C) 24, 48, 72 and 96 h after infection with NDV-BC (B) or NDV-BC/S (C) at MOI of 0.001 PFU. Cell lysates were prepared at the indicated time points post-infection and subjected to SDS-PAGE/Western blot analysis using NDV-specific and  $\beta$ -actin specific antibodies. HPI: h post-infection.

tissues after IN/IT immunization of non-human primates with NDV detected the virus in the lungs [10], but not in the nasal turbinates (A.B., B.R.M. and P.L.C., unpublished data). In addition, NDV replicated inefficiently in the lower respiratory tract when administered IN compared to the combined IN/IT routes (Fig. 2). Thus, it appears that, in contrast to the human viruses, avian NDV replicates poorly in the upper respiratory tract of primates, a property that could account for its reduced immunogenicity.

One possible explanation might be a lower density of NDV receptors in the upper respiratory tract of primates, as compared to the lower respiratory tract, and therefore a lower level of replication of the virus after IN inoculation. For example, low transmissibility of highly pathogenic H5N1 avian influenza virus in humans was suggested to be related to the lack of its receptor, sialic acid molecules linked to galactose by an  $\alpha$ -2,3-linkage, in the human upper respiratory tract [20]. Sialic acid also serves as a receptor for NDV receptor-binding protein HN; however, NDV appears to be less restricted than influenza virus in its requirements for certain modifications of the sialic acid molecule receptors [reviewed in [21]], and therefore this explanation seems unlikely.

Another possibility is that NDV replicates poorly in the upper respiratory tract of primates due to the lower temperature at that site, reflecting the adaptation of the virus to birds which, as already noted, have a higher body temperature. The idea that NDV is restricted in the upper respiratory tract due to its lower temperature is supported by the significant reduction in NDV-BC plaque size observed in cell culture during incubation performed at lower temperatures characteristic of the upper respiratory tract in primates; in contrast, no reduction was observed for HPIV3, a human respiratory pathogen (Fig. 7). Moreover, the production of virus during single- and multi-cycle growth experiments was strongly reduced at 32 °C for NDV-BC and NDV-BC/S but not for HPIV3 (Fig. 8). This was associated with reduced and delayed production of intracellular NDV antigen at 32 °C (Fig. 9). The observation that the replication of HPIV3 was not reduced at 32 °C suggests that the

reduced expression and replication of NDV at this reduced temperature is an intrinsic property of the virus rather than an artifact due to a reduced cellular metabolism. Thus, the ability of human viruses such as human influenza, respiratory syncytial virus, and parainfluenza viruses to efficiently replicate in the upper respiratory tract provides for spread to the lower respiratory tract, in which dendritic cells and other antigen-presenting cells are abundantly present. In contrast, we suggest that the inefficient antigen expression and reduced virus production of NDV in the upper respiratory tract of primates results in reduced spread the lower respiratory tract and reduced immune stimulation.

Two important conclusions for the development of NDV-vectored human vaccines can be made from this study. First, since IN delivery alone appeared to be ineffective in a primate model, nebulizer delivery of these vaccines to the lower respiratory tract may be a viable option for subsequent clinical trials. Nebulizer delivery of the measles vaccine to children was found to be safe, effective and inexpensive [25]. Second, since mesogenic and modified lentogenic strains of NDV appeared to be almost equally immunogenic and equally protective, the choice of strain for development of human vaccines should be based on factors other than immunogenicity. Issues such as safety for humans and for the bird population, as well as the ability to grow the virus to high titers in substrates approved for human vaccine production [reviewed in [4]] will be critical considerations when moving forward into clinical trials with these vaccine candidates.

#### Acknowledgements

We thank Elizabeth M. Williams and Lawrence J. Faucette for support of the IHC studies, Brad Finneyfrock and Anthony Cook of Bioqual, Inc. for their assistance with primate studies, and Ernest Williams and Fatemeh Davoodi for assistance with HAI and ELISA assays. This project was funded as a part of the Intramural Research Program of NIAID, NIH.

#### References

- [1] Bukreyev A, Skiadopoulos MH, Murphy BR, Collins PL. Nonsegmented negative-strand viruses as vaccine vectors. *J Virol* 2006;80(November (21)):10293–306.
- [2] Peeters BP, de Leeuw OS, Koch G, Gielkens AL. Rescue of Newcastle disease virus from cloned cDNA: evidence that cleavability of the fusion protein is a major determinant for virulence. *J Virol* 1999;73(June (6)):5001–9.
- [3] Panda A, Huang Z, Elankumaran S, Rockemann DD, Samal SK. Role of fusion protein cleavage site in the virulence of Newcastle disease virus. *Microb Pathog* 2004;36(January (1)):1–10.
- [4] Bukreyev A, Collins PL. Newcastle disease virus as a vaccine vector for humans. *Curr Opin Mol Ther* 2008;10(February (1)):46–55.
- [5] Nakaya T, Cros J, Park MS, Nakaya Y, Zheng H, Sagrera A, et al. Recombinant Newcastle disease virus as a vaccine vector. *J Virol* 2001;75(December (23)):11868–73.
- [6] Nakaya Y, Nakaya T, Park MS, Cros J, Imanishi J, Palese P, et al. Induction of cellular immune responses to simian immunodeficiency virus gag by two recombinant negative-strand RNA virus vectors. *J Virol* 2004;78(September (17)):9366–75.
- [7] Martinez-Sobrido L, Gitiban N, Fernandez-Sesma A, Cros J, Mertz SE, Jewell NA, et al. Protection against respiratory syncytial virus by a recombinant Newcastle disease virus vector. *J Virol* 2006;80(February (3)):1130–9.
- [8] DiNapoli JM, Kotelkin A, Yang L, Elankumaran S, Murphy BR, Samal SK, et al. Newcastle disease virus, a host range-restricted virus, as a vaccine vector for intranasal immunization against emerging pathogens. *Proc Natl Acad Sci USA* 2007;104(June (23)):9788–93.
- [9] DiNapoli JM, Yang L, Suguian Jr A, Elankumaran S, Dorward DW, Murphy BR, et al. Immunization of primates with a Newcastle disease virus-vectored vaccine via the respiratory tract induces a high titer of serum neutralizing antibodies against highly pathogenic avian influenza virus. *J Virol* 2007;81(November (21)):11560–8.
- [10] Bukreyev A, Huang Z, Yang L, Elankumaran S, St Claire M, Murphy BR, et al. Recombinant Newcastle disease virus expressing a foreign viral antigen is attenuated and highly immunogenic in primates. *J Virol* 2005;79(November (21)):13275–84.
- [11] Bukreyev A, Lamirande EW, Buchholz UJ, Vogel LN, Elkins WR, St Claire M, et al. Mucosal immunisation of African green monkeys (*Cercopithecus aethiops*) with an attenuated parainfluenza virus expressing the SARS coronavirus spike protein for the prevention of SARS. *Lancet* 2004;363(June (9427)):2122–7.

- [12] Reed LJ, Muench H. A simple method of estimating fifty per cent endpoints. *Am J Epidemiol* 1938;27:493–7.
- [13] McAuliffe J, Vogel L, Roberts A, Fahle G, Fischer S, Shieh WJ, et al. Replication of SARS coronavirus administered into the respiratory tract of African Green, rhesus and cynomolgus monkeys. *Virology* 2004;330(December (1)):8–15.
- [14] Keck T, Leiacker R, Riechelmann H, Rettinger G. Temperature profile in the nasal cavity. *The Laryngoscope* 2000;110(April (4)):651–4.
- [15] Graham BS, Perkins MD, Wright PF, Karzon DT. Primary respiratory syncytial virus infection in mice. *J Med Virol* 1988;26(October (2)):153–62.
- [16] Clements ML, Betts RF, Murphy BR. Advantage of live attenuated cold-adapted influenza A virus over inactivated vaccine for A/Washington/80 (H3N2) wild-type virus infection. *Lancet* 1984;1(March (8379)):705–8.
- [17] Karron RA, Wright PF, Belshe RB, Thumar B, Casey R, Newman F, et al. Identification of a recombinant live attenuated respiratory syncytial virus vaccine candidate that is highly attenuated in infants. *J Infect Dis* 2005;191(April (7)):1093–104.
- [18] Karron RA, Wright PF, Newman FK, Makhene M, Thompson J, Samorodin R, et al. A live human parainfluenza type 3 virus vaccine is attenuated and immunogenic in healthy infants and children. *J Infect Dis* 1995;172(6):1445–50.
- [19] Bertley FM, Kozlowski PA, Wang SW, Chappelle J, Patel J, Sonuyi O, et al. Control of simian/human immunodeficiency virus viremia and disease progression after IL-2-augmented DNA-modified vaccinia virus Ankara nasal vaccination in nonhuman primates. *J Immunol* 2004;172(March (6)):3745–57.
- [20] Shinya K, Ebina M, Yamada S, Ono M, Kasai N, Kawaoka Y. Avian flu: influenza virus receptors in the human airway. *Nature* 2006;440(March (7083)):435–6.
- [21] Villar E, Barroso IM. Role of sialic acid-containing molecules in paramyxovirus entry into the host cell: a minireview. *Glycoconj J* 2006;23(February (1–2)):5–17.
- [22] Murphy BR, Sly DL, Tierney EL, Hosier NT, Massicot JG, London WT, et al. Reassortant virus derived from avian and human influenza A viruses is attenuated and immunogenic in monkeys. *Science* 1982;218(December (4579)):1330–2.
- [23] Karron RA, Belshe RB, Wright PF, Thumar B, Burns B, Newman F, et al. A live human parainfluenza type 3 virus vaccine is attenuated and immunogenic in young infants. *Pediatr Infect Dis J* 2003;22(May (5)):394–405.
- [24] Sears SD, Clements ML, Betts RF, Maassab HF, Murphy BR, Snyder MH. Comparison of live, attenuated H1N1 and H3N2 cold-adapted and avian-human influenza A reassortant viruses and inactivated virus vaccine in adults. *J Infect Dis* 1988;158(December (6)):1209–19.
- [25] Bennett JV, Fernandez de Castro J, Valdespino-Gomez JL, Garcia-Garcia Mde L, Islas-Romero R, Echaniz-Aviles G, et al. Aerosolized measles and measles-rubella vaccines induce better measles antibody booster responses than injected vaccines: randomized trials in Mexican schoolchildren. *Bull WHO* 2002;80(10):806–12.